

Nonadiabatic evolution and thermodynamics of time-dependent open quantum system

Dan Wang¹ and Dazhi Xu^{1,*}

¹*Center for Quantum Technology Research and Key Laboratory of Advanced Optoelectronic Quantum Architecture and Measurements (MOE), School of Physics, Beijing Institute of Technology, Beijing 100081, China*

We investigate the dynamic evolution and thermodynamic process of a driven quantum system immersed in a finite-temperature heat bath. A Born-Markovian quantum master equation is formally derived for the time-dependent system with discrete energy levels. This quantum master equation can be applied to situations with a broad range of driving speed and bath temperature, thus can be used to study the finite-time quantum thermodynamics even when the nonadiabatic transition and dissipation coexist. The dissipative Landau-Zener model is thoroughly analyzed as an example, whose population evolution and transition probability reveal the importance of the competition between driving and dissipation beyond the adiabatic regime. Moreover, local maximums of irreversible entropy production occur at intermediate sweep velocity and finite temperature, which the low-dissipation model cannot describe.

I. INTRODUCTION

The open quantum system with time-dependent Hamiltonian simultaneously incorporates the coherent driving and the unavoidable environment noise; therefore, it can describe an increasingly broad range of physical systems controlled by the outside agents. The related problems include quantum transport [1], adiabatic quantum computation [2–5], optimal quantum control [6], and dissipative many-body systems [7–10], etc. Especially, the recent development of quantum thermodynamics boosts the research on time-dependent open systems [11–13].

Although efforts have been made for years to develop the appropriate description of the dissipative quantum dynamics with drive [14], no method is justified for all the situations. The slow-driven and periodical-driven systems are the two cases studied most, and formalisms based on the adiabatic master equation [15, 16] and Floquet’s theory [17–20] have been widely employed, respectively. Moreover, various numerical methods are proposed in terms of this issue, such as quasiadiabatic propagator path integral (QUAPI) [21], influence functional formalism [22], short-iterative Lanczos method [23], hierarchical equations of motion [24], quantum trajectories [25], and variational method [26, 27].

However, a general master equation is still needed, especially when the dissipation and nonadiabatic transition are comparable, the case of which usually occurs in dissipative systems with energy-level avoided crossing. Based on the assumption that the driving changes slowly compared with the bath correlation time, a Markovian master equation is proposed and applied to the dissipative Landau-Zener (LZ) model [28]. Indeed, this assumption is unnecessary, and the validity of the master equation is not constrained by the adiabatic condition, as pointed

out in Ref. [29] with an elaborate discussion on the definitions of different dynamic time scales their relations.

In this article, we derive a time-dependent quantum master equation (TDQME) for the systems with discrete energy levels. With the help of Nakajima–Zwanzig projective method [30] in the adiabatic frame of reference, this master equation is justified beyond adiabatic approximation. The advantage of this approach is that the nonadiabatic transition and the dissipation are completely decoupled in the equation; thus, the magnitudes and the time scales of these two crucial factors can be separately considered, which offers us great convenience to understand and even control the driven dissipative quantum systems. The time evolution and transition probability of the dissipative LZ model are calculated for demonstration. These results indicate our method can be used beyond the adiabatic condition and verify the conclusions in Ref. [29].

Furthermore, we can straightforwardly evaluate the average of thermodynamic quantities such as heat, work, and entropy in the nonequilibrium processes. The dependence of the irreversible entropy production on the total evolution time determines the trade-off relation between efficiency and output power of heat engine [31–33], which is generally linear in the low-dissipation regime [34–36]. Beyond the low-dissipation regime, we reveal that the irreversible entropy production changes nonmonotonically with the sweep velocity and temperature in the context of dissipative LZ model. Therefore, equipped with the TDQME, one can extend the optimal control of the finite-time quantum thermodynamic processes [37] to the more wide parameter regime and explore the more with profound physical phenomena.

The paper is arranged as follows. In Sec. II, we formally derive the TDQME. In Sec. III, the dissipative LZ system is served as an example, the dynamics and LZ probability of which are calculated. In Sec. IV, we study the finite-time thermodynamics of the dissipative LZ problem. In Sec. V, we briefly summarize our results and discuss the possible further work.

* dzxu@bit.edu.cn

II. TDQME IN ADIABATIC FRAME OF REFERENCE

In deriving the master equation for a time-independent system, we usually carry out the secular approximation according to the system eigenvalues drop the fast oscillatory terms. Then the resulted dissipation rate $\gamma(E_{ij})$ is a function of the energy-level difference E_{ij} between the two related eigenstates $|i\rangle$ and $|j\rangle$ [30]. This approach is often generalized to the time-dependent open quantum system by substituting the time-independent E_{ij} in $\gamma(E_{ij})$ with the instantaneous eigenvalue difference $E_{ij}(t)$. This naive approach requires that the system Hamiltonian changes slowly. The word ‘‘slowly’’ here has two folds of meaning: 1) the adiabatic theorem [38] is satisfied such that all the nonadiabatic transitions can be safely neglected; 2) the system changes slowly compare with the bath correlation time, such that the dissipative rate can change following the instantaneous eigenvalues. In order to find a quantum master equation that is justified for the arbitrary driving protocol and wide range of driving speed, working in the adiabatic frame of reference is a convenient choice.

A. Adiabatic frame of reference

Generally, a time-dependent open system is described by the Hamiltonian

$$H(t) = H_S(t) + H_B + V, \quad (1)$$

where $H_S(t)$ is the system Hamiltonian, H_B is the heat bath Hamiltonian, and V describes the system-bath interaction. We assume V is weak and all the time-dependent terms are taken into account by $H_S(t)$. The system Hamiltonian can be diagonalized as

$$H_S(t) = \sum_n E_n(t) |n(t)\rangle \langle n(t)|, \quad (2)$$

where $|n(t)\rangle$ the instantaneous eigenvector, and $E_n(t)$ the corresponding eigenvalue. Under the adiabatic approximation, the unitary evolution of a time-dependent system with Hamiltonian $H_S(t)$ and initial state $|n(t_0)\rangle$ is described as

$$|\psi_n(t)\rangle = e^{i\eta_n(t) + i\xi_n(t)} |n(t)\rangle, \quad (3)$$

where we define the dynamic and adiabatic phase factors

$$\eta_n(t) = - \int_{t_0}^t E_n(\tau) d\tau, \quad (4)$$

$$\xi_n(t) = i \int_{t_0}^t \langle n(\tau) | \dot{n}(\tau) \rangle d\tau. \quad (5)$$

Here we denote $|\dot{n}(\tau)\rangle \equiv \frac{d}{d\tau} |n(\tau)\rangle$ and set $\hbar = k_B = 1$.

The adiabatic frame of reference is defined by the operator

$$U(t) = \sum_n |\psi_n(t)\rangle \langle n(t_0)| \otimes e^{-iH_B t}. \quad (6)$$

The unitarity of $U(t)$ can be easily proved from the orthogonal completeness of $|\psi_n(t)\rangle$. $U(t)$ maps the time-dependent state $|\psi_n(t)\rangle$ to the instantaneous eigenstate $|n(t_0)\rangle$ of time t_0 , which can be arbitrarily chosen for convenience. We also incorporate the transformation of the heat bath in $U(t)$; then the transformed total Hamiltonian is given by

$$\begin{aligned} \tilde{H}(t) &= U^\dagger(t) H(t) U(t) - iU^\dagger(t) \frac{d}{dt} U(t) \\ &\equiv \tilde{H}_S(t) + \tilde{V}(t). \end{aligned} \quad (7)$$

Here the transformed system Hamiltonian reads

$$\tilde{H}_S(t) = \sum_{n \neq m} \alpha_{nm}(t) |n(t_0)\rangle \langle m(t_0)|, \quad (8)$$

where

$$\alpha_{nm}(t) = -ie^{-i\phi_{nm}(t)} \langle n(t) | \dot{m}(t) \rangle, \quad (9)$$

and $\phi_{nm}(t) \equiv \phi_n(t) - \phi_m(t)$, $\phi_n(t) \equiv \eta_n(t) + \xi_n(t)$. It can be seen from Eq. (8) that $\tilde{H}_S(t)$ only includes the nonadiabatic transitions, i.e., the transitions between the different instantaneous eigenstates. Moreover, the nonadiabatic transition coefficient $\alpha_{nm}(t)$ is proportional to $\langle n(t) | \dot{m}(t) \rangle$, whose magnitude usually increases with the driving speed. Therefore, $\tilde{H}_S(t)$ can be neglected when the adiabatic theorem is satisfied. Otherwise, we should consider its contribution to the dissipative dynamics of the driven open quantum system.

The transformed system-bath interaction is written as

$$\tilde{V}(t) = U^\dagger(t) V U(t), \quad (10)$$

which becomes time-dependent now. It is worth noticing that we should keep all the rotating wave and counter-rotating wave terms in the system-bath coupling V to ensure the secular approximation is carried out correctly in the adiabatic frame of reference.

B. Nakajima–Zwanzig projective approach

We follow the standard Nakajima–Zwanzig projective operator method [30] to derive the TDQME, such that the nonadiabatic transition and dissipation can be considered in the same framework. In the adiabatic frame of reference defined above, the quantum Liouville equation reads

$$\frac{d}{dt} \tilde{\rho}(t) = -i[\tilde{H}(t), \tilde{\rho}(t)] \equiv \mathcal{L}(t)[\tilde{\rho}(t)]. \quad (11)$$

Here $\tilde{\rho}(t)$ is the density operator of the total system in the adiabatic frame, it relates to the operator $\rho(t)$ in the original frame by $\tilde{\rho}(t) = U^\dagger(t) \rho(t) U(t)$. The Liouville superoperator $\mathcal{L}(t)$ can be decomposed into two parts $\mathcal{L} = \mathcal{L}_0 + \mathcal{L}_I$, where

$$\mathcal{L}_0[\tilde{\rho}(t)] = -i[\tilde{H}_S(t), \tilde{\rho}(t)], \quad (12)$$

$$\mathcal{L}_I[\tilde{\rho}(t)] = -i[\tilde{V}(t), \tilde{\rho}(t)]. \quad (13)$$

Then \mathcal{L}_0 describes the nonadiabatic evolution, and \mathcal{L}_I describes the system-bath interaction which should be treated perturbatively.

The projective operator \mathcal{P} is defined as

$$\mathcal{P}\tilde{\rho}(t) = \text{Tr}_B[\tilde{\rho}(t)] \otimes \rho_B \equiv \tilde{\rho}_S(t) \otimes \rho_B. \quad (14)$$

We can see \mathcal{P} maps $\tilde{\rho}(t)$ to a direct product the reduced density operators of system $\tilde{\rho}_S(t)$ and heat bath ρ_B . As the system-bath coupling is weak, it is reasonable to assume the heat bath is always in thermal equilibrium state $\rho_B = \exp(-\beta H_B)/\text{Tr}[\exp(-\beta H_B)]$. The orthogonal projective operator \mathcal{Q} is defined by

$$\mathcal{Q}\tilde{\rho}(t) = \tilde{\rho}(t) - \mathcal{P}\tilde{\rho}(t). \quad (15)$$

\mathcal{P} and \mathcal{Q} satisfy the relations $\mathcal{P}^2 = \mathcal{P}$, $\mathcal{Q}^2 = \mathcal{Q}$ and $\mathcal{P}\mathcal{Q} = \mathcal{Q}\mathcal{P} = 0$. We also assume that the expectation value of odd orders of $\tilde{V}(t)$ is zero, which can be written with superoperators as $\mathcal{P}\mathcal{L}_I(t_1)\mathcal{L}_I(t_2)\cdots\mathcal{L}_I(t_{2n+1})\mathcal{P} = 0$.

The quantum Liouville equation can be decomposed into two coupled equations by acting \mathcal{P} and \mathcal{Q} on Eq. (11) as

$$\frac{d}{dt}\mathcal{P}\tilde{\rho}(t) = \mathcal{P}\mathcal{L}(t)\mathcal{P}\tilde{\rho}(t) + \mathcal{P}\mathcal{L}(t)\mathcal{Q}\tilde{\rho}(t), \quad (16)$$

$$\frac{d}{dt}\mathcal{Q}\tilde{\rho}(t) = \mathcal{Q}\mathcal{L}(t)\mathcal{P}\tilde{\rho}(t) + \mathcal{Q}\mathcal{L}(t)\mathcal{Q}\tilde{\rho}(t). \quad (17)$$

Formally integrate Eq. (17), we obtain

$$\mathcal{Q}\tilde{\rho}(t) = \mathcal{G}(t, t_0)\mathcal{Q}\tilde{\rho}(t_0) + \int_{t_0}^t ds\mathcal{G}(t, s)\mathcal{Q}\mathcal{L}(s)\mathcal{P}\tilde{\rho}(s), \quad (18)$$

where the Green's function $\mathcal{G}(t, s)$ is defined as

$$\mathcal{G}(t, s) = \text{T}_{\leftarrow} \exp\left[\int_s^t d\tau\mathcal{Q}\mathcal{L}(\tau)\right], \quad (19)$$

and T_{\leftarrow} is the chronological time operator indicating the time argument increases from right to left. Taking Eq. (18) into Eq. (16) we can have

$$\frac{d}{dt}\mathcal{P}\tilde{\rho}(t) = \mathcal{P}\mathcal{L}(t)\mathcal{P}\tilde{\rho}(t) + \int_{t_0}^t ds\mathcal{K}(t, s)\tilde{\rho}(s), \quad (20)$$

where we define the convolution kernel operator

$$\mathcal{K}(t, s) = \mathcal{P}\mathcal{L}(t)\mathcal{G}(t, s)\mathcal{Q}\mathcal{L}(s)\mathcal{P}. \quad (21)$$

In deriving Eq. (20), we also use the Born approximation by assuming the initial state is a direct product state $\tilde{\rho}(t_0) = \tilde{\rho}_S(t_0) \otimes \rho_B$, such that $\mathcal{Q}\tilde{\rho}(t_0) = 0$. With the help of the facts $\mathcal{P}\mathcal{L}_I(t)\mathcal{P} = 0$ and $\mathcal{L}_0(t)\mathcal{Q} = \mathcal{Q}\mathcal{L}_0(t)$, we only keep the master equation to the second order of \mathcal{L}_I and approximately write

$$\mathcal{K}(t, s) \approx \mathcal{P}\mathcal{L}_I(t)\text{T}_{\leftarrow} e^{\int_s^t d\tau\mathcal{L}_0(\tau)}\mathcal{L}_I(s)\mathcal{P}. \quad (22)$$

Further, we use the Markovian approximation by substituting the integral variable $s \rightarrow t - s$ in Eq. (20) and

Eq. (22), and assume $\tilde{\rho}(t - s) \approx \tilde{\rho}(t)$ considering that the system density operator changes slightly within the time scale of the bath correlation time τ_B . Thus, we have

$$\begin{aligned} & \int_{t_0}^t ds\mathcal{K}(t, s)\tilde{\rho}(s) \\ & \approx \int_0^{t-t_0} ds\mathcal{P}\mathcal{L}_I(t)\text{T}_{\rightarrow} e^{\int_0^s d\tau\mathcal{L}_0(t-\tau)}\mathcal{L}_I(t-s)\mathcal{P}\tilde{\rho}(t). \end{aligned} \quad (23)$$

The exponential superoperator on the right side of the above equation can be written explicitly as

$$\text{T}_{\rightarrow} e^{\int_0^s d\tau\mathcal{L}_0(t-\tau)}\hat{O} = \tilde{R}(s)\hat{O}\tilde{R}^\dagger(s), \quad (24)$$

where \hat{O} stands for an arbitrary operator and

$$\tilde{R}(s) = \text{T}_{\rightarrow} \exp\left[-i \int_0^s d\tau\tilde{H}_S(t-\tau)\right]. \quad (25)$$

As can be seen from the dissipative LZ model below, Eq. (23) is proportional the bath correlation function, which quickly decays within the small time scale τ_B . Therefore, $\tilde{R}(s)$ contributes to Eq. (23) mainly during $0 \lesssim s \lesssim \tau_B$, such that we can safely approximate $\tilde{R}(s) \approx 1$, which is equivalent to assume

$$|\langle n(t)|\dot{m}(t)\rangle| \ll \tau_B^{-1}. \quad (26)$$

This condition could be easily satisfied, even if the adiabatic condition [38] is no longer justified.

Combine Eqs. (20,23,26) and trace over the bath degrees of freedom, we finally obtain the general form of the TDQME:

$$\frac{d}{dt}\tilde{\rho}_S(t) = \mathcal{L}_0[\tilde{\rho}_S(t)] + \mathcal{L}_B[\tilde{\rho}_S(t)], \quad (27)$$

where \mathcal{L}_0 is defined in Eq. (12) and \mathcal{L}_B is

$$\mathcal{L}_B[\tilde{\rho}_S(t)] = - \int_0^{t-t_0} ds\text{Tr}_B[\tilde{V}(t), [\tilde{V}(t-s), \tilde{\rho}_S(t) \otimes \rho_B]]. \quad (28)$$

The reduced density operator of the system can be obtained by solving Eq. (27) and then transform back into the original frame by $\rho_S(t) = \text{Tr}_B[U(t)\tilde{\rho}_S(t)U^\dagger(t)]$. The transformation $U(t)$ takes the responsibility of adiabatic evolution. If there is no nonadiabatic transition or dissipation, $U(t)$ will adiabatically rotate the system following the instantaneous eigenstates.

It should be mentioned that, as indicated in Ref. [29], the TDQME in the weak system-bath coupling case is actually not constrained by the condition (26) and can be applied to the situation with more significant nonadiabatic transitions. Briefly speaking, the violation of (26) implies the nonadiabatic transition is quite strong, such that the \mathcal{L}_B is negligible regardless how it is derived. We will illustrate this point in the following section with an example of the dissipative LZ problem.

III. DISSIPATIVE LZ SYSTEM

A. TDQME for linear driven two-level system

The linear driven two-level system interacting with a bosonic bath is an ideal model to demonstrate how to apply the TDQME, as it is both simple enough and contains almost all the essential ingredients of dissipative open systems. This model is also a good playground to study the finite-time quantum thermodynamics. If we focus on the physics around the avoid crossing point, this model is well-known as the LZ model with Hamiltonian

$$H_S(t) = vt\sigma_z + \epsilon\sigma_x, \quad (29)$$

where v is the sweep velocity and ϵ is the tunneling amplitude. The Pauli operators $\sigma_{x,z}$ are defined in the diabatic basis $|\uparrow\rangle$ and $|\downarrow\rangle$ as $\sigma_x = |\uparrow\rangle\langle\downarrow| + |\downarrow\rangle\langle\uparrow|$ and $\sigma_z = |\uparrow\rangle\langle\uparrow| - |\downarrow\rangle\langle\downarrow|$. The instantaneous eigenstates are

$$|e(t)\rangle = \cos\frac{\theta_t}{2}|\uparrow\rangle + \sin\frac{\theta_t}{2}|\downarrow\rangle, \quad (30)$$

$$|g(t)\rangle = -\sin\frac{\theta_t}{2}|\uparrow\rangle + \cos\frac{\theta_t}{2}|\downarrow\rangle, \quad (31)$$

where $\tan\theta_t = \epsilon/(vt)$, and the corresponding eigenvalues are

$$E_e(t) = -E_g(t) = \sqrt{v^2t^2 + \epsilon^2}. \quad (32)$$

The instantaneous energy levels are illustrated in Fig. (1). It is easy to show the Berry's phases $\xi_{e,g}(t)$ are all zero as

$$\langle e(t)|\dot{e}(t)\rangle = \langle g(t)|\dot{g}(t)\rangle = 0. \quad (33)$$

The effect of finite Berry's phase on the dissipative dynamics is also an interesting problem [39, 40] but will not be discussed in the current work. The strength of nonadiabatic transition (or the LZ transition) is

$$\langle e(t)|\dot{g}(t)\rangle = -\langle g(t)|\dot{e}(t)\rangle = \frac{\epsilon v/2}{v^2t^2 + \epsilon^2}. \quad (34)$$

Eq. (34) is a Lorentzian line shape as a function of t with maximum $v/(2\epsilon)$ and width $2\tau_{LZ}$, here $\tau_{LZ} = \epsilon/v$ is the time scale in which the LZ transition dominates the dynamics. If the sweep velocity is very fast, the nonadiabatic transition appears like a pulse with large amplitude and width $2\tau_{LZ}$.

The bath Hamiltonian H_B and the system-bath coupling V are

$$H_B = \sum_k \omega_k a_k^\dagger a_k, \quad (35)$$

and

$$V = \sigma_x \otimes \sum_k g_k (a_k^\dagger + a_k), \quad (36)$$

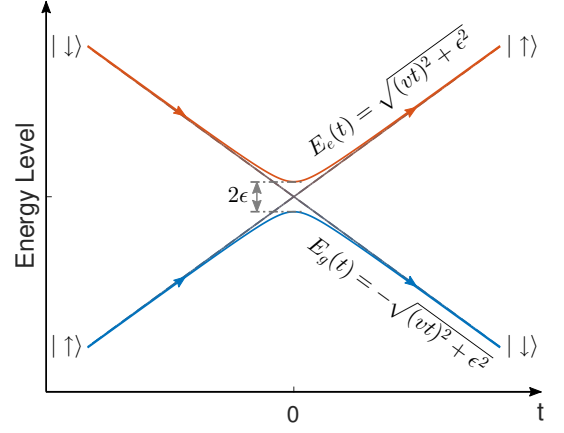


Figure 1. Schematic illustration of the LZ model. The minimal energy gap at $t = 0$ is 2ϵ . The time-dependent eigenvalues $E_{e,g}(t)$ are plotted with solid lines. In the adiabatic regime, the basis of the system transform from $|\uparrow\rangle(|\downarrow\rangle)$ at $t = -\infty$ to $|\downarrow\rangle(|\uparrow\rangle)$ at $t = \infty$ following the instantaneous eigenstates.

where a_k is the bosonic annihilation operator of the bath harmonic mode with frequency ω_k , g_k is the coupling strength. For simplicity, we only consider the case that the bath is transversely coupled with the two-level system via operator σ_x in the main text, the longitudinal σ_z -coupling case is briefly discussed in Appendix A. The linear combination of these two kinds of coupling is discussed in Ref. [41].

Apply the unitary transformation defined in (6), we obtain

$$\tilde{H}_S(t) = \alpha_{eg}(t)\hat{\sigma}_+ + \text{h.c.}, \quad (37)$$

and

$$\tilde{V}(t) = \tilde{\sigma}_x(t) \otimes B(t), \quad (38)$$

where $B(t) = \sum_k g_k (a_k^\dagger e^{i\omega_k t} + a_k e^{-i\omega_k t})$ and

$$\tilde{\sigma}_x(t) = \sin\theta_t \hat{\sigma}_z + \cos\theta_t [e^{-i\phi_{eg}(t)} \hat{\sigma}_+ + \text{h.c.}]. \quad (39)$$

Here the Pauli operators $\hat{\sigma}_{x,y,z,\pm}$ are defined in the basis $\{|e(t_0)\rangle, |g(t_0)\rangle\}$, for example, $\hat{\sigma}_+ = |e(t_0)\rangle\langle g(t_0)|$.

After take Eqs. (38,39) into Eq. (28), we can further use the secular approximation to neglect the fast oscillating terms, such as the ones containing factor $e^{\pm i\phi_{eg}(t)}$ or $e^{\pm i\phi_{eg}(t-s)}$. Then the dissipation superoperator can be expressed as

$$\begin{aligned} \mathcal{L}_B[\tilde{\rho}_S(t)] = & -i[S_+(t)\hat{\sigma}_+\hat{\sigma}_- + S_-(t)\hat{\sigma}_-\hat{\sigma}_+, \tilde{\rho}_S(t)] \\ & -\Gamma_+(t) (\{\hat{\sigma}_+\hat{\sigma}_-, \tilde{\rho}_S(t)\} - 2\hat{\sigma}_-\tilde{\rho}_S(t)\hat{\sigma}_+) \\ & -\Gamma_-(t) (\{\hat{\sigma}_-\hat{\sigma}_+, \tilde{\rho}_S(t)\} - 2\hat{\sigma}_+\tilde{\rho}_S(t)\hat{\sigma}_-) \\ & -2\Gamma_z(t) [\tilde{\rho}_S(t) - \hat{\sigma}_z\tilde{\rho}_S(t)\hat{\sigma}_z], \end{aligned} \quad (40)$$

where the energy-level shift $S_{\pm}(t)$, relaxation rate $\Gamma_{\pm}(t)$

are dephasing rate $\Gamma_z(t)$ are given by

$$S_{\pm}(t) = \cos \theta_t \int_0^{t-t_0} ds \cos \theta_{t-s} \text{Im}[C(s)e^{\pm i\Delta(t,s)}], (41)$$

$$\Gamma_{\pm}(t) = \cos \theta_t \int_0^{t-t_0} ds \cos \theta_{t-s} \text{Re}[C(s)e^{\pm i\Delta(t,s)}], (42)$$

$$\Gamma_z(t) = \sin \theta_t \int_0^{t-t_0} ds \sin \theta_{t-s} \text{Re}[C(s)]. (43)$$

Here $\Delta(t,s) = 2 \int_0^s d\tau \sqrt{v^2(t-\tau)^2 + \epsilon^2}$ and $C(s)$ is the bath correlation function

$$\begin{aligned} C(s) &\equiv \text{Tr}_B[B(t)B(t-s)\rho_B] \\ &= \frac{1}{\pi} \int_0^{\infty} d\omega J(\omega) \left[\coth\left(\frac{\beta\omega}{2}\right) \cos(\omega s) - i \sin(\omega s) \right], \end{aligned} (44)$$

where the system-bath coupling spectral density is defined as $J(\omega) = \pi \sum_k g_k^2 \delta(\omega - \omega_k)$. In this work, we assume $J(\omega)$ is an Ohmic spectral with an exponential cutoff $J(\omega) = \pi\gamma\omega e^{-\omega/\omega_c}$, where γ is the constant characterizing the system-bath coupling strength, and ω_c is the cutoff frequency. With such setting, the bath correlation function can be calculated as

$$C(s) = \gamma\omega_c^2 \left[\frac{2\text{Re}[\psi^{(1)}(\frac{1}{\beta\omega_c} + \frac{is}{\beta})]}{(\beta\omega_c)^2} + \frac{1}{(s\omega_c + i)^2} \right] (45)$$

with $\psi^{(1)}(z)$ the trigamma function. We can also choose $J(\omega)$ to be an Ohmic spectral with Lorentz-Drude cutoff and obtain the analytical form of $C(s)$ with the help of Matsubara expansion, which will not introduce any qualitative difference with the current work. However, the convergence speed of Matsubara expansion is much slower in the low temperature.

B. Time evolution

The two most important and competitive ingredients of the dissipative LZ system, LZ transition and dissipation, are now separately described in Eq. (27) by the unitary evolution $\mathcal{L}_0[\tilde{\rho}_S(t)]$ and non-unitary evolution $\mathcal{L}_B[\tilde{\rho}_S(t)]$, respectively. The unraveling of the dynamic processes helps us to clearly see how LZ transition and dissipation contribute in different time scales.

We plot $|\alpha_{eg}(t)|$, $\Gamma_+(t)$ and $\Gamma_z(t)$ as functions of the rescaled time t/τ_{LZ} in Fig. 2 for different sweep velocities $v/\epsilon^2 = 0.1, 1$ and 10 , at both high time temperature $T = 25\epsilon$ and low temperature $T = \epsilon$. Both $\Gamma_+(t)$ and $\Gamma_z(t)$ decrease with temperature, while $|\alpha_{eg}(t)|$ is temperature independent. Consistent with our discussion in Sec. IIIA, the Lorentzian line shape of $|\alpha_{eg}(t)|$ lies right at the avoid-crossing point $t = 0$, where there is a sharp decline of $\Gamma_+(t)$. The height of $|\alpha_{eg}(t)|$ linearly increases with the sweep velocity, when it goes into the nonadiabatic regime $v/\epsilon^2 > 1$ the LZ transition overwhelms

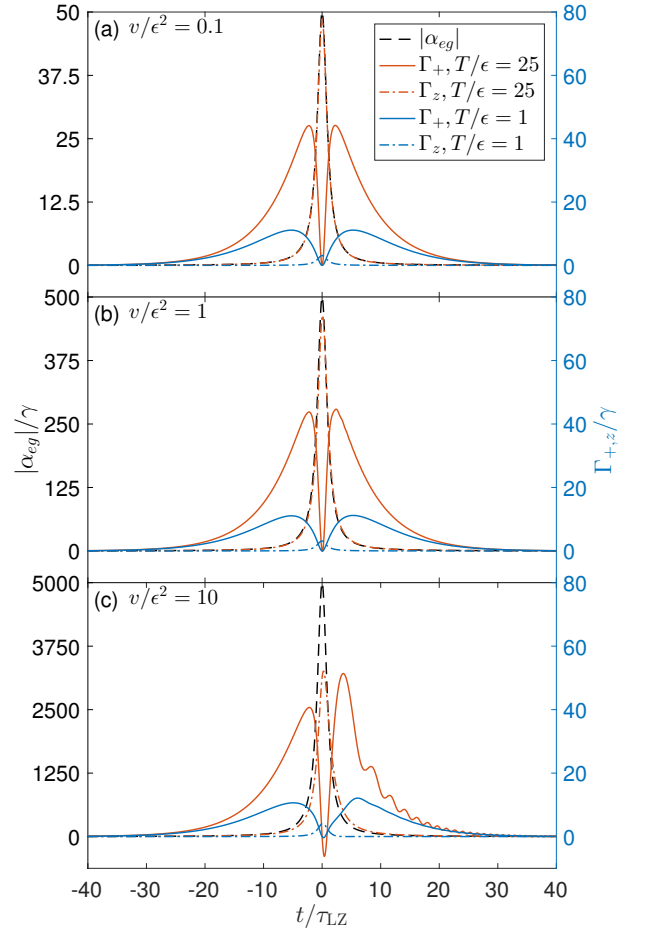


Figure 2. The strength of nonadiabatic transition $|\alpha_{eg}(t)|$, relaxation rate $\Gamma_+(t)$, and dephasing rate $\Gamma_z(t)$ as functions of evolution time t . Different sweep velocities are chosen in the (a) slow ($v/\epsilon^2 = 0.1$), (b) intermediate ($v/\epsilon^2 = 1$), and (c) fast ($v/\epsilon^2 = 10$) regimes. The nonadiabatic transition $|\alpha_{eg}(t)|$ (black dashed line) is a Lorentzian peak with width $2\tau_{LZ}$ and maximum $v/(2\epsilon)$. The relaxation rate $\Gamma_+(t)$ has a dip around $t = 0$, and its magnitude decreases with temperature ($T/\epsilon = 25$ for orange solid line and $T/\epsilon = 1$ for blue solid line). The dephasing rate $\Gamma_z(t)$ (dot-dashed lines) appears in the same time scale as $|\alpha_{eg}(t)|$, but its magnitude is much smaller. Here we set $\gamma = 0.001\epsilon$ and $\omega_c = 10\epsilon$.

the dissipation. The relaxation rate $\Gamma_+(t)$ has two maximums located around $t \approx \pm 2\tau_{LZ}$, beyond which $\Gamma_+(t)$ exponentially decreases to zero in a time scale about $2\omega_c/v$. The curves of $\Gamma_-(t)$ are very similar to but lower than $\Gamma_+(t)$, thus are not presented here.

In the adiabatic regime ($v/\epsilon^2 \lesssim 1$), $\Gamma_+(t)$ is almost a symmetric function of t as shown in Fig. 2(a). This is because when $\tau_{LZ} \gg \tau_B$, we can approximately write Eq. (42) as

$$\Gamma_+(t) \approx \cos^2 \theta_t J[2E_e(t)] \{n[2E_e(t)] + 1\}, (46)$$

$$\Gamma_-(t) \approx \cos^2 \theta_t J[2E_e(t)] n[2E_e(t)], (47)$$

where $n(\omega) = 1/[\exp(\beta\omega) - 1]$, the expressions on the right are obvious even functions of time. Eqs. (46,47) are

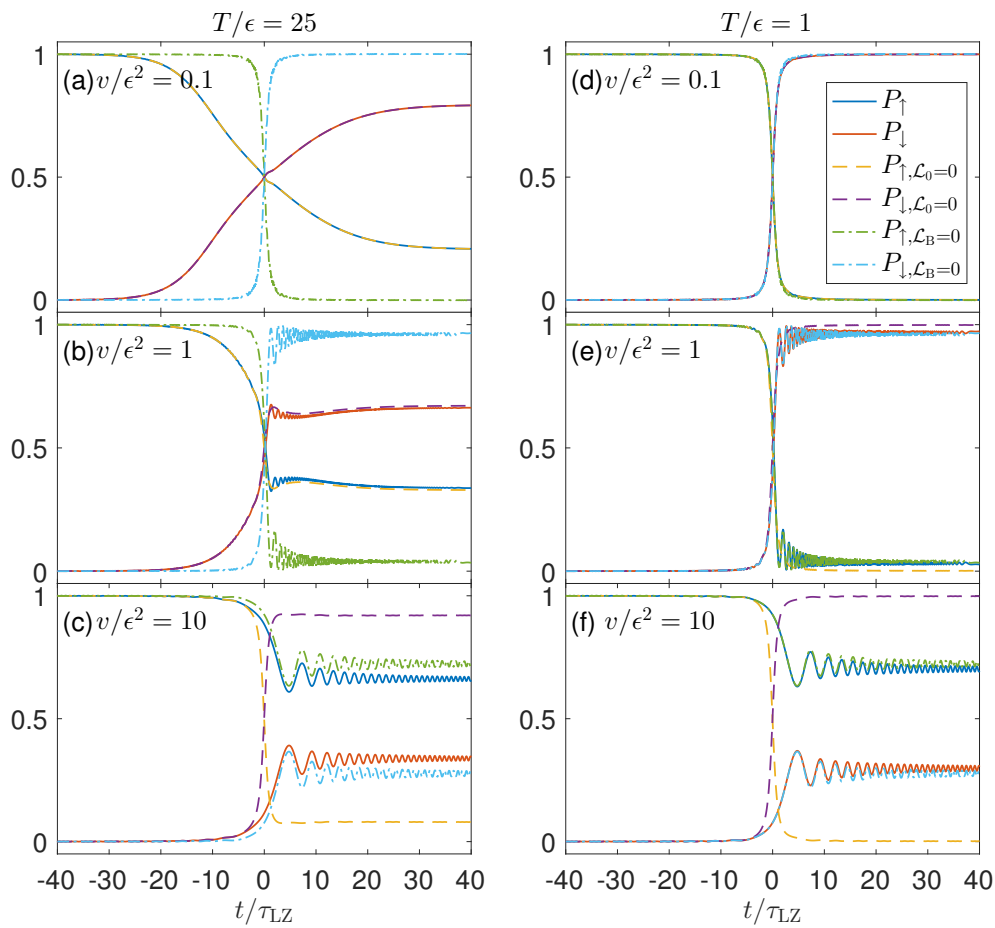


Figure 3. Time evolution of diabatic states populations of the dissipative LZ model. The initial state is chosen as $|\uparrow\rangle$. The evolution starts at $t_0 = -40\tau_{\text{LZ}}$ and ends at $t_f = 40\tau_{\text{LZ}}$. From top to bottom, the two subplots in each row correspond to $v/\epsilon^2 = 0.1, 1$ and 10 , respectively; the left (right) panel is the high (low) temperature case with $T/\epsilon = 25$ ($T/\epsilon = 1$). The populations $P_{\uparrow,\downarrow}(t)$ calculated by the TDQME are plotted with solid lines. As comparison, we also plot the populations evolution in the cases without the nonadiabatic transition ($\mathcal{L}_0 = 0$) and without the dissipation ($\mathcal{L}_B = 0$). Other parameters are the same as Fig. 2.

usually directly employed in the adiabatic master equation [33, 42], but they are no longer justified if v rises into the nonadiabatic regime and should be calculated according to Eq. (42). As shown in Fig. 2(c) with $v/\epsilon^2 = 10$, two peaks of $\Gamma_+(t)$ becomes asymmetry and $\Gamma_+(t)$ slightly oscillates on top of an exponential decay when $t \gtrsim 2\tau_{\text{LZ}}$ at $T = 25\epsilon$. In this nonadiabatic case, $\Gamma_+(t)$ becomes negative for a very short time as soon as $t > 0$. The appearance of negative $\Gamma_+(t)$ means the relaxation turns into pumping. However, this anomalous will not induce any significant result as it only lasts for an instant, and the LZ transition is overwhelming simultaneously.

The dephasing rate $\Gamma_z(t)$ is approximately proportional to $\sin^2\theta_t$ and contributes along with $|\alpha_{eg}(t)|$ in the time domain. The effect of this term is to reduce the coherence between the states $|e(t_0)\rangle$ and $|g(t_0)\rangle$, or equivalently between diabatic basis $|\uparrow\rangle$ and $|\downarrow\rangle$ as we set the initial evolution time $t_0 \ll 0$ in the following calculation. The energy-level shift $S_{\pm}(t)$ is not shown here, considering its influence on the dynamics is negligible if

the system-bath coupling is weak.

The time evolution of the populations $P_{\zeta}(t) = \langle \zeta | \rho_S(t) | \zeta \rangle$ ($\zeta = \uparrow, \downarrow$) are shown in Fig. 3. The sweep velocities of the subplots in each row are $v/\epsilon^2 = 0.1, 1$ and 10 from top to bottom, respectively. The left (right) panel shows the high (low) temperature cases with $T/\epsilon = 25$ ($T/\epsilon = 1$). The time evolution starts at $t_0 = -40\tau_{\text{LZ}}$ with the initial state $|\psi(t_0)\rangle = |\uparrow\rangle$ and ends at $t_f = 40\tau_{\text{LZ}}$, outside this period the dynamics becomes trivial because everything decays to zero as shown in Fig. 2. In contrast, we also plot two sets of curves: $P_{\uparrow(\downarrow), \mathcal{L}_0=0}$ represents the population calculated by manually closing the nonadiabatic transitions $\mathcal{L}_0[\tilde{\rho}_S(t)] = 0$, while $P_{\uparrow(\downarrow), \mathcal{L}_B=0}$ is the population in the original LZ problem without dissipation ($\mathcal{L}_B[\tilde{\rho}_S(t)] = 0$).

As shown in Fig. 3(a)(d) with $v/\epsilon^2 = 0.1$ in the adiabatic regime, $P_{\uparrow(\downarrow)}(t)$ coincides very well with the curve $P_{\uparrow(\downarrow), \mathcal{L}_0=0}(t)$, because the dissipation $\mathcal{L}_B[\tilde{\rho}_S(t)]$ dominates the time evolution and the LZ transition can be neglected. When the bath temperature is high [as $T/\epsilon = 25$

in Fig. 3(a)], the thermal excitation prevents $|\uparrow\rangle$ from completely transferring into $|\downarrow\rangle$, thus $P_{\downarrow}(t_f)$ is smaller than 1, which is quite different from the original unitary LZ problem. However, if the temperature is low as $T/\epsilon = 1$, the heat bath intends to cool the system to the new ground state after passing the avoid crossing point, whose effect is coincidence with the adiabatic evolution, thus all the three sets of curves overlap in Fig. 3(d).

The effects of nonadiabatic LZ transition emerge when the sweep velocity gradually increases to $v/\epsilon^2 = 1$. As shown in Fig. 3(b)(e), $P_{\uparrow(\downarrow)}(t > 0)$ is slightly higher (lower) than $P_{\uparrow(\downarrow), \mathcal{L}_0=0}(t > 0)$ because the LZ transition prefers to reserve more population on the initial state $|\uparrow\rangle$. Fast oscillation with small amplitude appears on $P_{\uparrow(\downarrow)}(t > 0)$, which is the typical signature of the LZ dynamics. If we further increase the sweep velocity to $v/\epsilon^2 = 10$, the dynamics of the dissipative LZ model are very similar to the original LZ model because of the relatively weak dissipation. The small disparity between $P_{\uparrow(\downarrow)}(t > 0)$ and $P_{\uparrow(\downarrow), \mathcal{L}_B=0}(t > 0)$ in Fig. 3(d) when $T/\epsilon = 25$ is the evidence of thermal excitation, which is barely noticeable in the low temperature case [Fig. 3(f)].

We should emphasize that the dissipative LZ system generally cannot relax to the instantaneous thermal equilibrium state $\rho_S^{\text{eq}}(t) \equiv e^{-H_S(t)/T}/\text{Tr}[e^{-H_S(t)/T}]$, because the dissipation stops when the time-dependent energy gap is much larger than the bath cut-off frequency ω_c . As a result, the system will evolve into a steady state with effective temperature higher than that of the heat bath. If we ignore the coherence, we can define a time-dependent effective temperature of the system as $T_{\text{eff}}(t) = 2E_e(t)/\ln[P_{\downarrow}(t)/P_{\uparrow}(t)]$, which increases with the growing v , $T_{\text{eff}}(t_f)$ even becomes negative when $v/\epsilon^2 = 10$ implying the populations are inverted $P_{\downarrow}(t_f) < P_{\uparrow}(t_f)$.

C. LZ probability

The LZ probability $P_{\text{LZ}}(v)$ lies in the heart of the LZ problem, which is defined by

$$P_{\text{LZ}}(v) = |\langle \downarrow | T_{\leftarrow} e^{-i \int_{-\infty}^{\infty} dt H_S(t)} | \uparrow \rangle|^2. \quad (48)$$

If we initially preparing the two-level system in the state $|\uparrow\rangle$ at $t_0 \rightarrow -\infty$, then let the system unitarily evolve to $t_f \rightarrow \infty$ governed by a linear driving $H_S(t)$, $P_{\text{LZ}}(v)$ gives the probability of finally finding the system in state $|\downarrow\rangle$, which has a well-known expression [43, 44] as

$$P_{\text{LZ}}(v) = 1 - \exp\left(-\frac{\pi\epsilon^2}{v}\right). \quad (49)$$

It is not only interesting but also of practical importance to study how the dissipation interferes the LZ transition, thus the open system version of LZ probability evokes a broad and long lasting interest [21, 41, 45–50]. In the open system, we can analogously define the LZ probability $P(v)$ by replacing the unitary evolution in

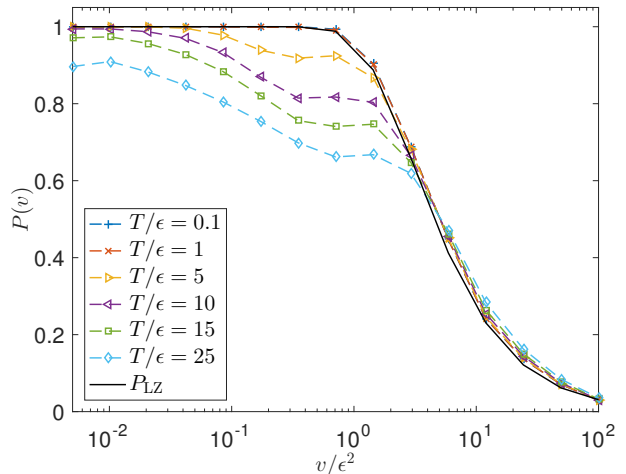


Figure 4. The LZ probability $P(v)$ with different temperatures. The TDQME results are presented in color markers for $T/\epsilon = 0.1, 1, 5, 10, 15,$ and 25 , while the black solid line is the LZ probability $P_{\text{LZ}}(v)$. $P(v)$ and $P_{\text{LZ}}(v)$ coincide well when $v/\epsilon^2 < 1$ and the temperature is low ($T/\epsilon = 0.1$ and 1). When the sweep velocity is large ($v/\epsilon^2 \gtrsim 10$), the nonadiabatic transition dominates the evolution, hence $P(v)$ at different temperatures approach to but are a little higher than $P_{\text{LZ}}(v)$, such small disparities are the results of dissipation and finally washed out at extremely large v . Nonmonotonic behavior of $P(v)$ appears around $v/\epsilon^2 = 1$ and $T/\epsilon \gtrsim 10$, when the nonadiabatic transition and dissipation are comparable in strength. Other parameters are the same as Fig. 2.

Eq. (48) by the dissipative dynamics described by the TDQME with initial state $\rho_S(t_0) = |\uparrow\rangle\langle\uparrow|$, i.e.,

$$P(v) = \langle \downarrow | \rho_S(t_f) | \downarrow \rangle. \quad (50)$$

We calculate $P(v)$ with $t_f = -t_0 \approx 100\tau_{\text{LZ}}$, such that the time evolution is long enough to cover all the nonadiabatic and dissipative processes. In Fig. 4, we plot both $P(v)$ at various temperatures and $P_{\text{LZ}}(v)$ with respect to the logarithmic of v . Except for the low temperature cases $T/\epsilon < 1$, in the adiabatic regime $P(v)$ decreases with increasing v . As we mentioned in the last subsection, the relaxation is active only in a time scale inverse to v , thus the system decouples with the heat bath at an earlier time as v increases before it is equilibrium, and more populations are left in $|\uparrow\rangle$. As the sweep velocity further increases into the region $v/\epsilon^2 \sim 1$, the gradually enhanced LZ transition starts to compete with dissipation and eventually dominates the evolution. Therefore, a local minimum of $P(v)$ appears around $v/\epsilon^2 \sim 1$ and then $P(v)$ quickly decreases with v increasing into LZ regime ($v/\epsilon^2 \gg 1$). The residual influence of the heat bath in the regime $1 \lesssim v/\epsilon^2 \lesssim 10$ is reflected by the small disparities of $P(v)$ above $P_{\text{LZ}}(v)$.

Let us mention that the nonmonotonicity of the LZ probability is more apparent in the case of longitudinal system-bath coupling than the transverse coupling case discussed here, in which the relaxation plays a more important role (see Appendix A). Our results obtained by

the TDQME method are well consistent with those calculated by QUAPI [41].

IV. FINITE-TIME THERMODYNAMICS

The above calculation suggests the TDQME is a useful tool to explore the finite-time thermodynamics of quantum systems with discrete energy levels. In the framework of quantum thermodynamics, the internal energy $U(t) = \text{Tr}[\rho_S(t)H_S(t)]$ and von Neumann entropy $S(t) = -\text{Tr}[\rho_S(t)\ln\rho_S(t)]$ are the functions of the system state at the present time, which are analogous to their classical counterparts. However, the input work $W(t)$ and the absorbed heat $Q(t)$ depend on the driving protocol. The work is defined as

$$W(t) = \int_{t_0}^t d\tau \text{Tr} \left[\rho_S(\tau) \frac{\partial H_S(\tau)}{\partial \tau} \right], \quad (51)$$

and heat can be obtained by the first law of thermodynamics as $Q(t) = \Delta U(t) - W(t)$, where $\Delta U(t) = U(t) - U(t_0)$ is the increase of internal energy.

The second law of thermodynamics tells us the entropy never decreases in a closed system. Accordingly, the total entropy production, usually termed as irreversible entropy production $\Delta S_{\text{irr}}(t)$ is always nonnegative and can be decomposed as

$$\Delta S_{\text{irr}}(t) = \Delta S(t) - \Delta S_e(t) \geq 0. \quad (52)$$

Here, $\Delta S(t) = S(t) - S(t_0)$ and $\Delta S_e(t) \equiv Q(t)/T$ is the entropy decrease of the heat bath due to the output heat current. In finite-time processes, the system is generally in the nonequilibrium state, and the irreversible entropy production $\Delta S_{\text{irr}}(t)$ serves to characterize the deviation of the system away from equilibrium [51, 52].

It is usually believed that the leading order of $\Delta S_{\text{irr}}(t)$ is inversely proportional to the total evolution time under the low-dissipation assumption, i.e., $\Delta S_{\text{irr}}(t_f) \propto 1/(t_f - t_0)$ [31], which is confirmed both theoretically [33, 35] and experimentally [36] in the system without energy level avoided crossing. The validity of low-dissipation assumption requires there should be no retard of equilibrium, which is easily violated in fast driving processes. To explore the behavior of $\Delta S_{\text{irr}}(t)$ in a more broad region, we start with the calculation of $\Delta S(t)$ and $\Delta S_e(t)$ in the dissipative LZ model. We initialize the system in a thermal equilibrium state $\rho_S(t_0) = e^{-\beta H_S(t_0)} / \text{Tr}[e^{-\beta H_S(t_0)}]$, and then let the system evolve from $t_0 = -40\tau_{\text{LZ}}$ to $t_f = 40\tau_{\text{LZ}}$, when the system finally approaches a nonequilibrium steady state.

In the large sweep velocity region ($v/\epsilon^2 \gtrsim 10$), the LZ system evolves in an almost unitary way with slight influence from the heat bath, as a result $\Delta S(t_f)$ and $\Delta S_e(t_f)$ quickly approach zero with growing v , as shown in Fig. 5(a) and (c). Even when the temperature is much higher than ϵ , for instance $T/\epsilon = 100$, the LZ transition is still hundreds of times larger than the dissipation during $t \in [-\tau_{\text{LZ}}, \tau_{\text{LZ}}]$, hence the dissipation can be safely

neglected. On the other hand, when the sweep velocity is small ($v/\epsilon^2 \lesssim 1$), the LZ transition becomes insignificant, such that the system tends to adiabatically follow its instantaneous eigenstates meanwhile exchanges heat with the bath. The smaller the sweep velocity is, the more population stays in the initial adiabatic basis, so the change of system entropy $\Delta S(t_f)$ decreases accordingly. In the intermediate region $1 \lesssim v/\epsilon^2 \lesssim 10$, the LZ transition and the adiabatic following compete with each other, which largely disturbs the population distribution and results in local maximums of $\Delta S(t_f)$.

Local maximums of $\Delta S(t_f)$ also appear when we change temperature and fix the sweep velocity [Fig. 5(b)]. In the low temperature limit as T/ϵ approaching 1, the dissipation is too weak to have substantial influence to the unitary evolution, thus $\Delta S(t_f)$ is decreasingly small. In the high temperature limit as $T/\epsilon \rightarrow 100$, the critical issue resulting small $\Delta S(t_f)$ relies on the fact that the entropy of a binary distribution changes less significantly when entropy is of larger value. Consequently, no matter how much the initial state populations are changed by the subsequent dynamics, $\Delta S(t_f)$ is bounded by $\ln 2 - S(t_0)$, which is very small for a high temperature initial equilibrium state.

The entropy flow $\Delta S_e(t_f)$ as functions of sweep velocity and temperature are presented in Fig. 5(c) and (d), respectively. In the large sweep velocity limit or high temperature limit, the $\Delta S_e(t_f)$ is also extremely small due to the similar reason as that of $\Delta S(t_f)$. We should mention that, $\Delta S_e(t_f)$ is small in high T limit also because $\Delta S_e(t_f)$ equals heat absorption rescaled by $1/T$. Furthermore, the heat absorption is positively related to the variation rate of the population difference between two instantaneous eigenstates, which is greatly suppressed at high T . More sophisticated behavior of $\Delta S_e(t_f)$ appears at low temperature ($T/\epsilon \lesssim 10$) in the intermediate sweep velocity region, which is consistent with the nonmonotonic region of $P(v)$ in Fig. 4, where the LZ transition is maximally intervened by dissipation.

The irreversible entropy production $\Delta S_{\text{irr}}(t_f)$ are plotted as functions of v and T in Fig. 6(a) and (b), respectively. Its behavior can be understood by combining the above results, which will not be repeated here. As shown in Fig. 6(a), $\Delta S_{\text{irr}}(t_f)$ linearly increases with v only in the region of low v ($v/\epsilon^2 < 1$) and high T ($T/\epsilon > 50$), beyond which $\Delta S_{\text{irr}}(t_f)$ shows nonmonotonic dependence on v . Linear proportional to v is equivalent with inversely proportional to $t_f - t_0$ in the current situation, which indicates the low-dissipation regime. The important thing about TDQME is, regardless of the low-dissipation assumption, now we can quantitatively determine in what conditions $\Delta S_{\text{irr}}(t_f)$ reaches the maximum or minimum, which lies in the heart of designing high efficiency thermodynamic cycles. It is worth noticing, the energy level avoid crossing can induce more profound dynamic and thermal phenomena, which should be paid enough attention to in the optimization problems in finite-time thermodynamics.

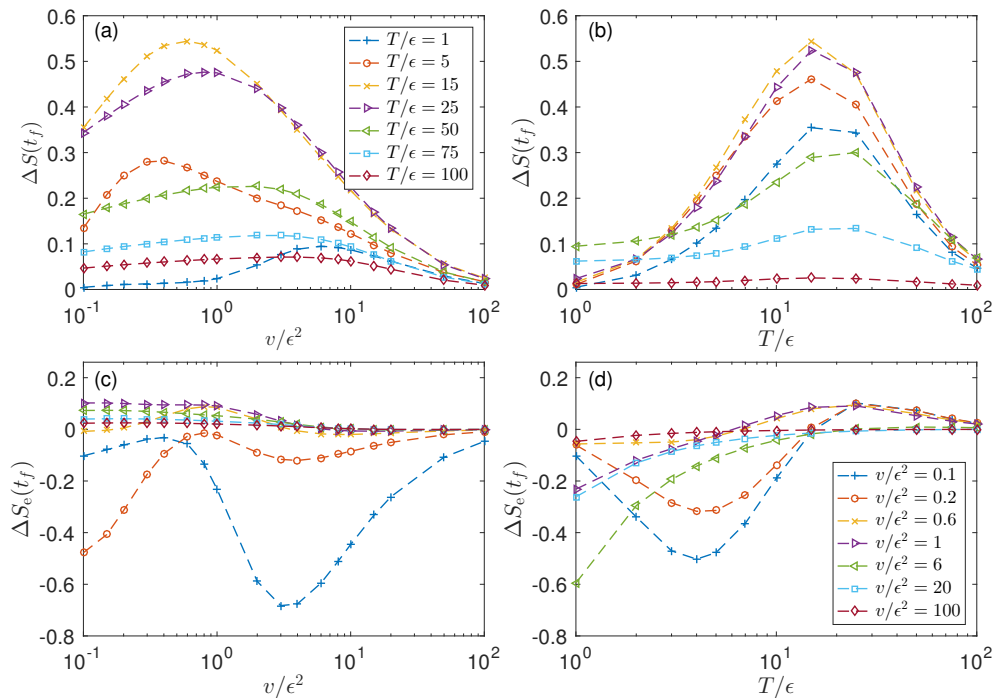


Figure 5. The change of entropy $\Delta S(t_f)$ and entropy flow $\Delta S_e(t_f)$ as functions of v in subplots (a)(c) and T in subplots (b)(d). The initial state is the instantaneous equilibrium state at $t_0 = -40\tau_{LZ}$. Other parameters are the same as Fig. 2.

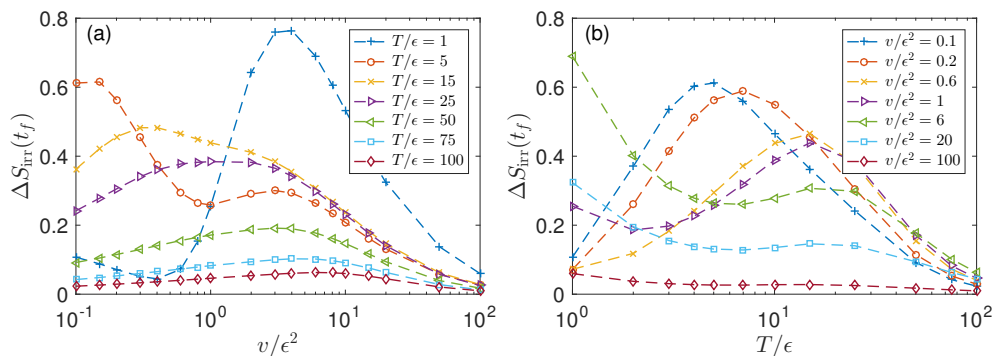


Figure 6. The irreversible entropy production $\Delta S_{irr}(t_f)$ as functions of (a) v and (b) T . The low-dissipation regime appears with low sweep velocities and high temperatures, where $\Delta S_{irr}(t_f)$ changes linearly with v . Other parameters are the same as Fig. 5.

V. CONCLUSIONS AND OUTLOOK

We have formally derived a Born-Markovian quantum master equation for the time-dependent open system in the adiabatic basis representation based on the Nakajima-Zwanzig projective operator method. Our formalism can be applied to arbitrary driving protocol with a broad range of driving speeds and is justified even beyond the adiabatic regime. Several authors have pointed out that the nonadiabatic transition and dissipation hardly dominate the system dynamics simultaneously; thus the adiabatic condition is not a necessary requirement in our approach. This idea is explicitly illustrated in our formalism by separating the Liouville oper-

ator into the nonadiabatic transition and the dissipation terms. Take the dissipative LZ system as example, we show that when the system is driven fast, the nonadiabatic transition overwhelms the dissipation. On the other hand, when the sweep velocity is decreasing, the nonadiabatic transition decreases in magnitude; meanwhile, it separates with the dissipation in the time domain. The validity of our approach has been checked by calculating the LZ probabilities with finite-temperature heat baths and compared with previous numerical results.

The competition between the time-dependent dissipation and nonadiabatic transition plays an essential role in determining the thermodynamic properties of finite-time processes, which is clearly revealed by the dissipative LZ

system. Our calculation show that in the case of system linearly passing through the avoid crossing point, the entropy, heat, and irreversible entropy change nonmonotonically with sweep velocity and bath temperature. The low-dissipation regime only appears with high temperature and slow driving, which is consistent with the usual understanding. However, our TDMQE is applicable in situations with parameters beyond the low-dissipation regime and can be used in the problems such as optimization of the performance of quantum Carnot cycle [53], and the distributions of the work and heat in stochastic quantum thermodynamics [42, 54–58].

ACKNOWLEDGMENTS

D. X. thanks Hui Dong and Jinfu Chen for helpful discussion. This study is supported by NSF of China (Grants No. 11705008 and Grants No. 12075025).

Appendix A: LZ probability with longitudinal system-bath coupling

In this appendix we present the results of dissipative LZ model with pure longitudinal system-bath coupling

$$V = \sigma_z \otimes \sum_k g_k (a_k^\dagger + a_k), \quad (\text{A1})$$

which after transformed into the adiabatic frame of reference reads $\tilde{V}(t) = \tilde{\sigma}_z(t) \otimes B(t)$ with

$$\tilde{\sigma}_z(t) = \cos \theta_t \hat{\sigma}_z - \sin \theta_t [e^{-i\phi_{eg}(t)} \hat{\sigma}_+ + \text{h.c.}]. \quad (\text{A2})$$

Eq. (A2) is similar with $\tilde{\sigma}_x(t)$ in Eq. (39) except for $\cos \theta_t$ and $\sin \theta_t$ interchanged. As a result, the relaxation only occurs within the time window $t \leq |\tau_{\text{LZ}}|$ in the longitudinal coupling case, while the pure dephasing occurs outside the time window. Recall the dissipative rates in Fig. 2, the relaxation in the transverse coupling case effectively exists for a longer time than that of the longitudi-

nal coupling case, thus causes more apparent dissipative effects.

We plot the LZ probability of the longitudinal system-bath coupling case in Fig. 7. There are two main difference comparing with the transverse coupling case: in the low sweep velocity regime the local minimums of $P(v)$ have smaller values and shift to smaller v ; on the other hand, $P(v)$ converges more quickly to $P_{\text{LZ}}(v)$ when $v/\epsilon^2 \gtrsim 1$. The simple explanation is that in the longitudinal coupling case, the relaxation occurs when the energy gap is very small as about 2ϵ , thus in the regime of low sweep velocity the bath intends to relax the two-level system with more evenly distributed populations on the instantaneous eigenstates at finite temperature, thus the $P(v)$ is smaller than that of the transverse coupling case; in the high sweep velocity regime, as the nonadiabatic transition and relaxation occur in the same time window and the former overwhelms the later, the influence of the heat bath is totally washed out regardless of temperature. Our results are consistent with the QUAPI results in Ref. [21, 41].

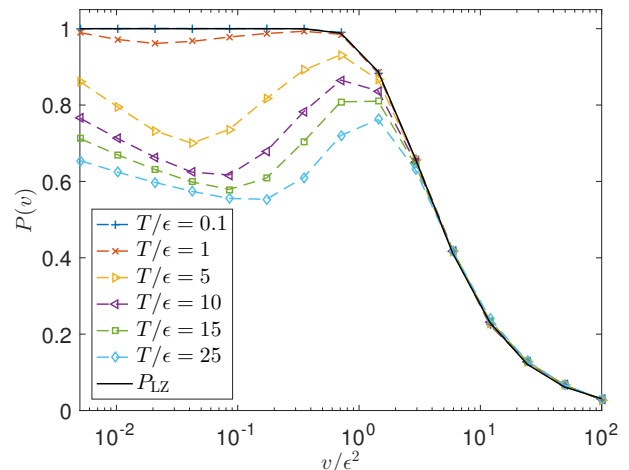


Figure 7. The LZ probability $P(v)$ of the longitudinal system-bath coupling case for various temperatures. The TDQME results are presented in color markers for $T/\epsilon = 0.1, 1, 5, 10, 15,$ and 25 , while the black solid line is the LZ probability $P_{\text{LZ}}(v)$. $P(v)$ and $P_{\text{LZ}}(v)$ coincide well when $v/\epsilon^2 \gtrsim 2$ for all the temperatures. Other parameters are the same as Fig. 4.

-
- [1] S. Kohler, J. Lehmann, and P. Hänggi, *Phys. Rep.* **406**, 379 (2005).
 - [2] A. M. Childs, E. Farhi, and J. Preskill, *Phys. Rev. A* **65**, 012322 (2002).
 - [3] M. H. S. Amin, P. J. Love, and C. J. S. Truncik, *Phys. Rev. Lett.* **100**, 060503 (2008).
 - [4] I. d. Vega, M. C. Bañuls, and A. Pérez, *New J. Phys.* **12**, 123010 (2010).
 - [5] N. G. Dickson, M. W. Johnson, M. H. Amin, R. Harris, F. Altomare, A. J. Berkley, P. Bunyk, J. Cai, E. M. Chap-

- ple, P. Chavez, F. Cioata, T. Cirip, P. deBuen, M. Drew-Brook, C. Enderud, S. Gildert, F. Hamze, J. P. Hilton, E. Hoskinson, K. Karimi, E. Ladizinsky, N. Ladizinsky, T. Lanting, T. Mahon, R. Neufeld, T. Oh, I. Perminov, C. Petroff, A. Przybysz, C. Rich, P. Spear, A. Tcaciuc, M. C. Thom, E. Tolkacheva, S. Uchaikin, J. Wang, A. B. Wilson, Z. Merali, and G. Rose, *Nat. Commun.* **4**, 1903 (2013).
- [6] P. R. Zulkowski and M. R. DeWeese, *Phys. Rev. E* **92**, 032113 (2015).

- [7] Y.-A. Chen, S. D. Huber, S. Trotzky, I. Bloch, and E. Altman, *Nat. Phys.* **7**, 61 (2011).
- [8] P. Nalbach, S. Vishveshwara, and A. A. Clerk, *Phys. Rev. B* **92**, 014306 (2015).
- [9] L. Arceci, S. Barbarino, D. Rossini, and G. E. Santoro, *Phys. Rev. B* **98**, 064307 (2018).
- [10] L. Pan, X. Chen, Y. Chen, and H. Zhai, *Nat. Phys.* **16**, 767 (2020).
- [11] M. Esposito, U. Harbola, and S. Mukamel, *Rev. Mod. Phys.* **81**, 1665 (2009).
- [12] M. Campisi, P. Hänggi, and P. Talkner, *Rev. Mod. Phys.* **83**, 771 (2011).
- [13] J. P. Pekola, *Nat. Phys.* **11**, 118 (2015).
- [14] E. B. Davies and H. Spohn, *J. Stat. Phys.* **19**, 511 (1978).
- [15] J. Vidal and J. Wudka, *Phys. Rev. A* **44**, 5383 (1991).
- [16] P. Solinas, M. Möttönen, J. Salmilehto, and J. P. Pekola, *Phys. Rev. B* **82**, 134517 (2010).
- [17] S. Kohler, T. Dittrich, and P. Hänggi, *Phys. Rev. E* **55**, 300 (1997).
- [18] D. W. Hone, R. Ketzmerick, and W. Kohn, *Phys. Rev. E* **79**, 051129 (2009).
- [19] G. B. Cuetara, A. Engel, and M. Esposito, *New J. Phys.* **17**, 055002 (2015).
- [20] S. Restrepo, J. Cerrillo, V. M. Bastidas, D. G. Angelakis, and T. Brandes, *Phys. Rev. Lett.* **117**, 250401 (2016).
- [21] P. Nalbach and M. Thorwart, *Phys. Rev. Lett.* **103**, 220401 (2009).
- [22] G. M. G. McCaul, C. D. Lorenz, and L. Kantorovich, *Phys. Rev. B* **95**, 125124 (2017).
- [23] L. M. Cangemi, V. Cataudella, M. Sassetti, and G. D. Filippis, *Phys. Rev. B* **100**, 014301 (2019).
- [24] Z. Sun, L. Zhou, G. Xiao, D. Poletti, and J. Gong, *Phys. Rev. A* **93**, 012121 (2016).
- [25] K. W. Yip, T. Albash, and D. A. Lidar, *Phys. Rev. A* **97**, 022116 (2018).
- [26] Z. Huang and Y. Zhao, *Phys. Rev. A* **97**, 013803 (2018).
- [27] V. Cavina, A. Mari, A. Carlini, and V. Giovannetti, *Phys. Rev. A* **98**, 052125 (2018).
- [28] P. Nalbach, *Phys. Rev. A* **90**, 042112 (2014).
- [29] M. Yamaguchi, T. Yuge, and T. Ogawa, *Phys. Rev. E* **95**, 012136 (2017).
- [30] H.-P. Breuer and F. Petruccione, *The Theory of Open Quantum Systems* (Oxford University Press, Great Clarendon Street, 2007).
- [31] M. Esposito, R. Kawai, K. Lindenberg, and C. V. d. Broeck, *Phys. Rev. Lett.* **105**, 150603 (2010).
- [32] V. Holubec and A. Ryabov, *J. Stat. Mech.* **2016**, 073204 (2016).
- [33] Y.-H. Ma, D. Xu, H. Dong, and C.-P. Sun, *Phys. Rev. E* **98**, 042112 (2018).
- [34] Z.-C. Tu, *Chinese Phys. B* **21**, 020513 (2012).
- [35] V. Cavina, A. Mari, and V. Giovannetti, *Phys. Rev. Lett.* **119**, 050601 (2017).
- [36] Y.-H. Ma, R.-X. Zhai, J. Chen, C. P. Sun, and H. Dong, *Phys. Rev. Lett.* **125**, 210601 (2020).
- [37] P. Abiuso and M. Perarnau-Llobet, *Phys. Rev. Lett.* **124**, 110606 (2020).
- [38] A. Messiah, *Quantum Mechanics* (Dunod, Paris, 1973).
- [39] R. S. Whitney, Y. Makhlin, A. Shnirman, and Y. Gefen, *Phys. Rev. Lett.* **94**, 070407 (2005).
- [40] G. D. Chiara, A. Łoziński, and G. M. Palma, *Eur. Phys. J. D* **41**, 179 (2007).
- [41] S. Javanbakht, P. Nalbach, and M. Thorwart, *Phys. Rev. A* **91**, 052103 (2015).
- [42] F. Liu, *Phys. Rev. E* **90**, 032121 (2014).
- [43] C. Zener, *Proc. R. Soc. A* **137**, 696 (1932).
- [44] L. D. Landau, *Phys. Z. Sowjetunion* **2**, 46 (1932).
- [45] M. Wilkinson, *J. Phys. Math. Gen.* **21**, 4021 (1988).
- [46] P. Ao and J. Rammer, *Phys. Rev. B* **43**, 5397 (1991).
- [47] Y. Kayanuma and H. Nakayama, *Phys. Rev. B* **57**, 13099 (1998).
- [48] K. Saito, M. Wubs, S. Kohler, Y. Kayanuma, and P. Hänggi, *Phys. Rev. B* **75**, 214308 (2007).
- [49] A. Dodin, S. Garmon, L. Simine, and D. Segal, *J. Chem. Phys.* **140**, 124709 (2014).
- [50] R. Chen, *Phys. Rev. B* **101**, 125426 (2020).
- [51] S. Vaikuntanathan and C. Jarzynski, *EPL* **87**, 60005 (2009).
- [52] M. Esposito and C. V. d. Broeck, *EPL* **95**, 40004 (2011).
- [53] Y.-H. Ma, D. Xu, H. Dong, and C.-P. Sun, *Phys. Rev. E* **98**, 022133 (2018).
- [54] P. Solinas, D. V. Averin, and J. P. Pekola, *Phys. Rev. B* **87**, 060508 (2013).
- [55] S. Suomela, P. Solinas, J. P. Pekola, J. Ankerhold, and T. Ala-Nissila, *Phys. Rev. B* **90**, 094304 (2014).
- [56] S. Gasparinetti, P. Solinas, A. Braggio, and M. Sassetti, *New J. Phys.* **16**, 115001 (2014).
- [57] K. Funo and H. T. Quan, *Phys. Rev. Lett.* **121**, 040602 (2018).
- [58] S. Suomela, J. Salmilehto, I. G. Savenko, T. Ala-Nissila, and M. Möttönen, *Phys. Rev. E* **91**, 022126 (2015).